VOL. 15, NO. 22, NOVEMBER 2020 ISSN 1819-6608
ARPN Journal of Engineering and Applied Sciences

www.arpnjournals.com

DOUBLE NITROGEN-DOPED CARBON TO SUPPORT FE-N-C CATALYST IN ELECTROCHEMICAL AND PHYSICAL PROPERTIES

Vuri Ayu Setyowati[1], Diah Susanti[2], Lukman Noerochim[2], Chen-Hao Wang[3] and Fauzan Abdul Aziz[1]
[1]Department of Mechanical Engineering, Institut Teknologi Adhi Tama Surabaya, Indonesia
[2]Institut Teknologi Sepuluh Nopember, Indonesia
[3]National Taiwan University of Science and Technology, Taiwan
E-Mail: vuri@itats.ac.id

ABSTRACT

The aims of this study is to analyze the new material substitute for Pt/C catalyst with the main material Fe as a metal precursor, graphite as carbon, and variations of nitrogen derived from organic compounds. The homogenous mixing generated a nitrogen-coated carbon surface after pyrolysis. Nitrogen and carbon were fixed in the ratio of 1:1 and mixed with the compound $FeCl_3.6H_2O$ dissolved with ethanol. The percentage of Fe was 7wt%. Pyrolysis was carried out at 700°C for 2 hours under N_2 atmosphere. The formation of new compounds after pyrolysis, such as FeS and Fe_2O_3, has a role to increase catalytic activity. The Fe-N (urea + PVP) -C catalyst has the largest CV and current density area compared to the Fe-N (urea) -C and Fe-C catalysts. These results are caused by the largest surface area of 7.239 m²/g of Fe-N (urea + PVP) -C and have a uniform distribution of nitrogen on the carbon surface as shown by the SEM observation image. In addition, the good electrochemical properties of the Fe-N (urea + PVP) -C catalyst due to the high nitrogen content of the EDX analysis of 2.97 wt% demonstrate it is possible to form nitrogen functional groups after pyrolysis.

Keywords: non-precious metal catalyst, electrochemical properties, double nitrogen source, physical properties.

INTRODUCTION

The development of green, sustainable energy storage has become important because of the increasing environmental problems caused by fossil fuels. Solar cell, fuel cell, batteries, and super capacitors are types of energy storage and storage technologies created to overcome the pollution and scarcity of nature resources. The oxygen reduction reaction (ORR) is the key to realizing the optimal performance of electrochemical energy conversion, such as batteries and fuel cells [1]. The oxygen reduction reaction (ORR) can be proceeded by two overall pathways in a direct 4-electron pathway and an indirect 2-electron pathway [2]. Platinum (Pt) has the most active catalyst on the desired 4-electron transfer ORR process. However, much of the research leads the development to replace the Pt loading using non-precious metals as electrocatalyst materials. Some of transitional metal and nitrogen can replace Pt to form a metal-nitrogen structure, such as the following sequence: Fe>Co>Cu>Mn>Ni. A non-precious metal catalyst (NPMC) was studied using a metal precursor mixed carbon and nitrogen source for pyrolysis. Setyowati *et al.* used polyaniline (PANI) and several iron precursors to study the differences in ORR activity. $FeCl_3$-PANI/C exhibited Fe-N4 structure and leads to high ORR activity because of high quaternary-type nitrogen [3].

NPMC used carbon as a support material because of the high electrical conductivity and stability in electrochemical condition. The porous structure is easily transferred and formed the active sites. N-doped carbon is derived into two groups, incorporating both nitrogen and transition [4] metal or simply a nitrogen atom into the carbon matrix [5]. N-doped carbon nanomaterial is one of the main types investigated for the enhancement of oxygen reduction reaction. The classification method for nitrogen doping of the carbon nanostructure are directly doping during synthesis of porous carbon nanostructure materials, called “in situ" doping, and post treatment of pre-synthesized carbon nanostructure with nitrogen containing precursor (N_2, NH_3, etc.), called “post” doping [6]. Jager *et al*. synthesized Fe-N/C using various N sources: urea (Urea), ethylenediaminetetraacetic acid disodium salt (EDTA), 1,10-phenanthroline (Phen), 2,2′-bipyridine (Bipyr) and in-house synthesized novel 1,3-di(1H-imidazol-1-yl)-2-propanol (DIPO), and concluded that the ORR increases in the following order: Fe+Urea/C < Fe+EDTA/C < Fe+DIPO/C ≤ Fe+Phen/C ≤ Fe+Bipyr/C in 0.1M KOH, as well as in 0.1M HClO4 electrolyte solutions [7].

Catalyst properties including high electrochemical stability, good electrical conductivity, and homogeneous particle distribution can be improved by high-temperature pyrolysis [8] [9] [10], chemical synthesis [11], and physical mixing treatments [12]. Catalytic activity directly attributed to temperature treatment. The activity recovery was observed from 200°C to 950°C. Acid washing, reheat treatment, and multiple acid washing-reheat treatment are used to determine suitable treatment for improving ORR. Range temperature of 200 to 300°C cannot be correlated to new sites formation. The ORR activity was shown after being treated at temperatures above 600°C [13]. Wu, Gang, *et.al* studied the effect of heating the temperature of the PANI-Fe-C catalyst from 400°C to 1000°C. Some analysis measurements were used to understand factor-attributed catalytic activity and FTIR characterized absorption bonding of the PANI-Fe-C before pyrolysis. The polymer chains also were determined. The relevant band disappears starting at 600°C, indicating that

the benzene-type and quinine type structure on PANI were decomposed [14]. Nitrogen levels and species were needed to control because they are responsible for enhancing the ORR activity. Takahiro Kondo, *et al.* studied the different types of nitrogen, such as pyrrolic, pyridinic, and graphitic N groups. ORR may result from the pyridinic N atoms. It has a larger electronegativity N atom, creating a carbon lattice to easily adsorb the O_2 molecule and facilitate the O=O bond breaking of O_2 [15]. Nitrogen doped carbon has the configuration of nitrogen that affects the catalytic activity. Therefore, it is important to improve the active N doped carbon to get a nitrogen bonding configuration in porous carbon[16]. Based on the view point of the nitrogen role for improving the catalytic activity, various nitrogen sources were used to synthesize N-doped carbon using Fe precursor by following pyrolysis method.

EXPERIMENTAL STUDY

Synthesis of Nitrogen Doped Carbon

Urea and Polivinil Pirolidon (PVP) were purchased from Merck product and were used as a nitrogen precursor. Graphite was used as the carbon support catalyst. There were two samples of nitrogen-containing catalyst and one sample without the addition of nitrogen. Carbon and nitrogen sources were mixed with ethanol solvent and stirred for 8 hours at room temperature. The mixture was filtered and washed by 2L of deionized water then heated at 80°C overnight. The obtained products were N(urea+PVP)-C, N(urea), and C without nitrogen.

Synthesis of Fe-N-C Catalyst

$FeCl_3.6H_2O$ (99+% purity, Merck) was used as the iron precursor, and Fe was fixed to 7wt% for all samples. $FeCl_3.6H_2O$ was dispersed in 20 mL of ethanol solvent and N-C powders were added to the iron solution. The mixture was put into an ultrasonic bath for 30 minutes. The solvent was removed and dried in a furnace. To improve the active site, pyrolysis was conducted at 700°C for 2 hours in N_2 atmosphere using 20°C/min as heating rate. The products of the catalyst were named as Fe- N(urea+PVP)-C, Fe-N(urea), and Fe-C as comparison.

Characterization

Fe- N(urea+PVP)-C, Fe-N(urea), and Fe- C were characterized in order to analyze the electrochemical and physical properties. CV was measured using potentiostat with the potential range of -0.15 V - 0.85 V in 0.1 M $HClO_4$ media. Physical characterizations consist of using the Scanning Electron Microscope (SEM) to identify the morphology, Energy Dispersive X-ray Spectroscopy (EDX) to analyze the element composition of catalyst, and X-ray diffraction (XRD) to determine compound or phases. The surface area was also measured by Brunauer-Emmett-Teller (BET) and FTIR to show the molecular structures.

RESULTS AND DISCUSSIONS

The electrochemical properties of prepared catalysts were measured by Cyclic Voltammetry (CV). As shown in Figure-1, ORR cathodic peaks appeared, indicating that the samples have active site [17]. Fe-N (urea+PVP)-C displayed the most positive ORR peak potential and the highest cathodic current density compared to Fe-C and Fe-N(urea)-C. This result indicates the highest ORR activity of the Fe-N (urea+PVP)-C catalyst and reveals that doping nitrogen has important influence for improving ORR activity [18].

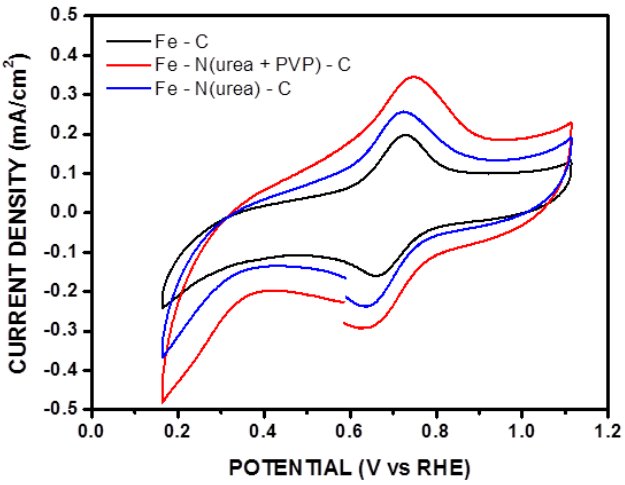

Figure-1. Cyclic Voltammetry of catalyst using various nitrogen compositions in 0.1M $HClO_4$ media measurement.

Table-1 summarizes the data of CV measurement. Fe-N (urea+PVP)-C catalyst has the largest area of CV curves and Fe-C catalyst is the smallest indicating the Fe-N (urea+PVP)-C capacity. Moreover, high current density of cathode belongs to the Fe-N(urea)-C catalyst. It is supposed that the value of current density in cathode is correlated with the surface area of the catalyst.

Table-1. The electrochemical properties of CV measurement.

Sample	Capacity (F)	E_p. Anode (V vs RHE)	I_p. Anode (mA/cm^2)	E_p. Cathode (V vs RHE)	I_p. Cathode (mA/cm^2)
Fe - C	0.0071	0.724	0.219	0.660	0.112
Fe - N(urea + PVP) - C	0.0133	0.740	0. 479	0.626	0.124
Fe - N(urea)-C	0.0087	0.721	0.325	0.640	0.130

SEM morphology in Figure-2 illustrates the differences of particulate shape. Catalyst without the addition of nitrogen source from urea and PVP promotes more agglomerates than nitrogen doped carbon catalyst. Nitrogen is deposited on carbon surface of Fe-N(urea)-C catalyst and is uniformly distributed to the carbon surface after PVP addition. Fe-N(urea-PVP)-C catalyst has a clear, porous structure, indicating some mesopores. This kind of structure facilitates the oxygen transport to active sites and the removal of water from the catalyst surface [19]. The presence of urea and PVP decomposed as a sacrificial pore-forming agent during the carbonization process, leaving the pores in the carbon matrix [20]. Herein the decomposition of urea leads the formation of porous structure. Fe-N(urea+PVP)-C catalyst has 7.239 m^2/g of surface area, which is higher than Fe-N(urea)-C of 3.633 m^2/g surface area. High surface area is obtained and can expose more active sites because it decreases the diffusion resistance and enhance the three-phase boundary of gas, electrolyte, and solid catalyst, which are both beneficial to improving the catalytic performance [21] [22].

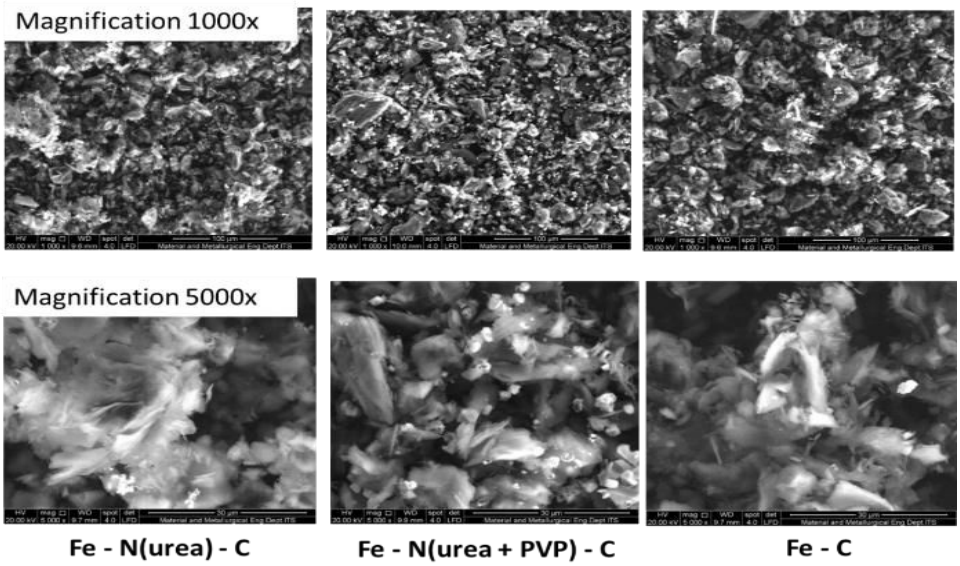

Figure-2. SEM image of the various catalyst using different component.

One of the most important factors for improving the catalytic activity is heat treatment. Non-precious metal catalyst developed pyrolysis at the desired temperature to improve the activity and stability of transition metal macrocycles for the ORR catalyst [23]. The diffraction pattern of XRD curves between pyrolyzed catalyst and without pyrolysis is shown in Figure 3. Pyrolyzed catalyst has the highest intensity of carbon peak without pyrolysis. Furthermore, pyrolyzed catalyst has a strong peak, indicating the iron compound exists in a catalyst such as FeS (JCPDS, PDF# 370477) at 33.25° and 49.5°, Fe_2O_3 (JCPDS, PDF# 391346) at 35.53°, 62.57 °, 64.17 °, and Fe_3C (JCPDS, PDF# 350772) at 54° and 77.56°, respectively. The presence of a new iron compound reveals that the heat treatment conducted generates many species consisting metal nitrogen species, metal oxide, and metal carbides [24] [25].

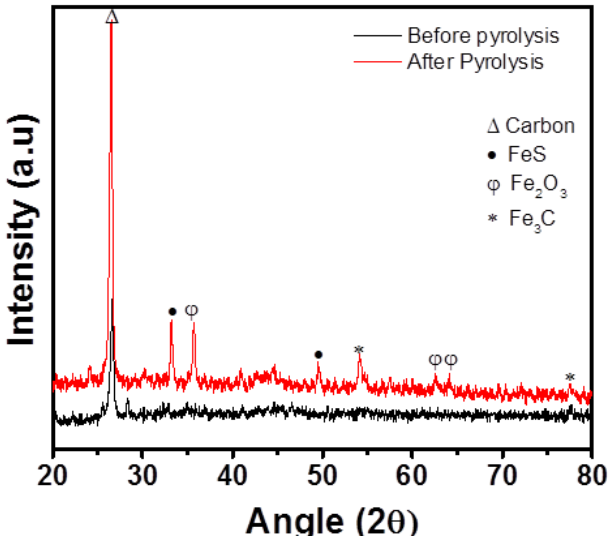

Figure-3. XRD pattern of Fe-N(urea-PVP)-C catalyst before and after pyrolysis.

Pyrolysis provides benefits in the process of graphitization. On catalysts, which are carried out before pyrolysis, have a carbon content of half of the carbon content after pyrolysis. Figure-4 shows the elemental composition of obtained catalyst. This proves that pyrolysis can form functional groups that are useful for improving catalytic activity. Nitrogen was not found in the catalyst before pyrolysis but could be analyzed for 2.97 wt% N elements after pyrolysis which showed that the pyrolysis process succeeded in forming a nitrogen group. The Cl element in the catalyst before pyrolysis is obtained from metal precursor $FeCl_3.6H_2O$ and can also be from the use of solvent HCl during the catalyst synthesis process. The condition of the pyrolysis carried out in a vacuum and flowed with argon gas aims to reduce the impurity in the sample so that there is no more presence of Cl in the catalyst after pyrolysis. O and Fe atoms have decreased levels after pyrolysis, indicating that iron interacts with amorphous carbon and promotes for surface rearrangement after pyrolysis [26] [27].

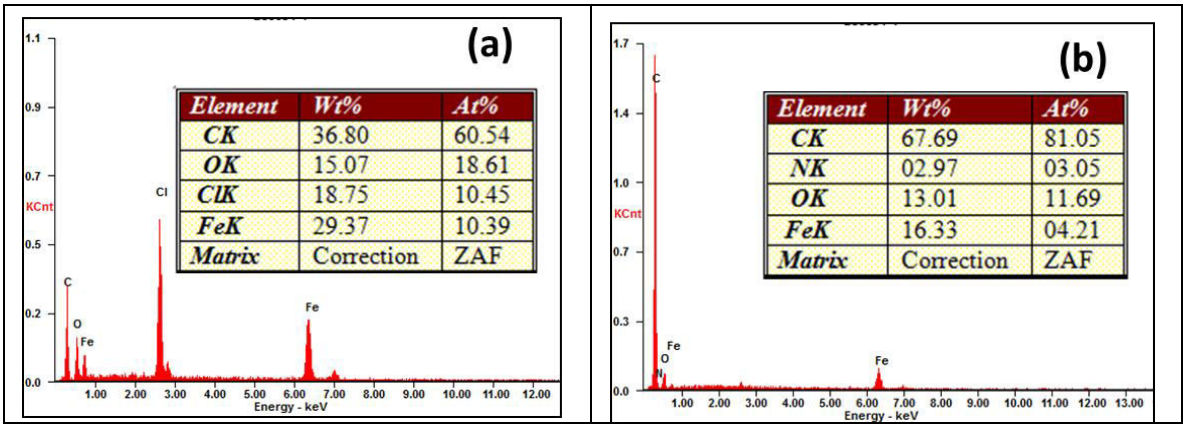

Figure-4. EDX spectra of catalyst (a) before and (b) after pyrolysis.

The existence of a new iron compound after pyrolysis is shown by Figure-5. Fe-C catalyst has a different peak from other samples for FeC compound in 45° of 2θ positions. Peak intensity of Fe-C catalyst is the lowest peak, compared to when nitrogen is added to the catalyst. Fe-N(urea+PVP)-C catalyst has the Fe_2O_3 and FeS compound. The presence of the FeS compound has the important role for synergetic increased catalytic activity. FeS can enhance the $E_{1/2}$ (half-wave potential) but lower the E_{onset} (onset potential). It can be concluded that the presence of FeS creates a reactive site to lower E_{onset} [28].

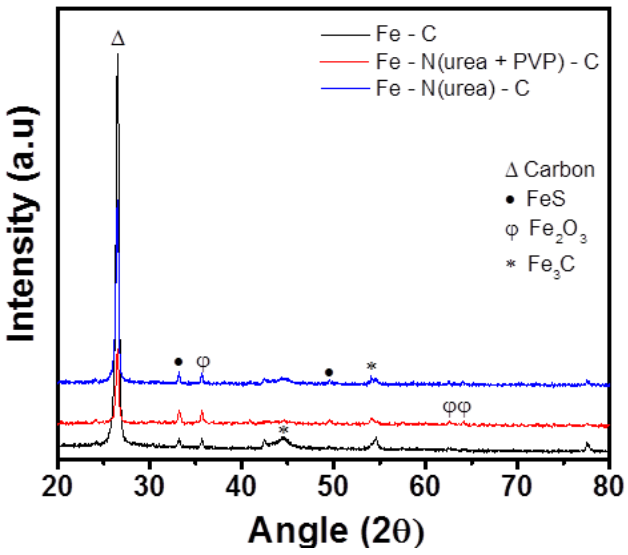

Figure-5. XRD pattern of the obtained catalyst using various compositions.

Catalysts with different composition variations contain different elements in the EDX test as shown by Figure-6. Fe-C catalyst has the highest carbon peak intensity compared to Fe-N (urea) -C and Fe-N (urea-PVP) -C catalyst. This high carbon peak shows that the most dominant crystalline carbon structure, Fe-N (urea) -C catalyst, does not have nitrogen so that the compounds formed from XRD curves are Fe_3C and Fe_2O_3. The high nitrogen content in the Fe-N (urea + PVP) -C catalyst shows that nitrogen groups have formed after the pyrolysis process, which can increase the active site. This can be seen in the CV image that Fe-N (urea + PVP) -C has greater capacity and current density at the cathode than Fe-C and Fe-N (urea) -C catalyst.

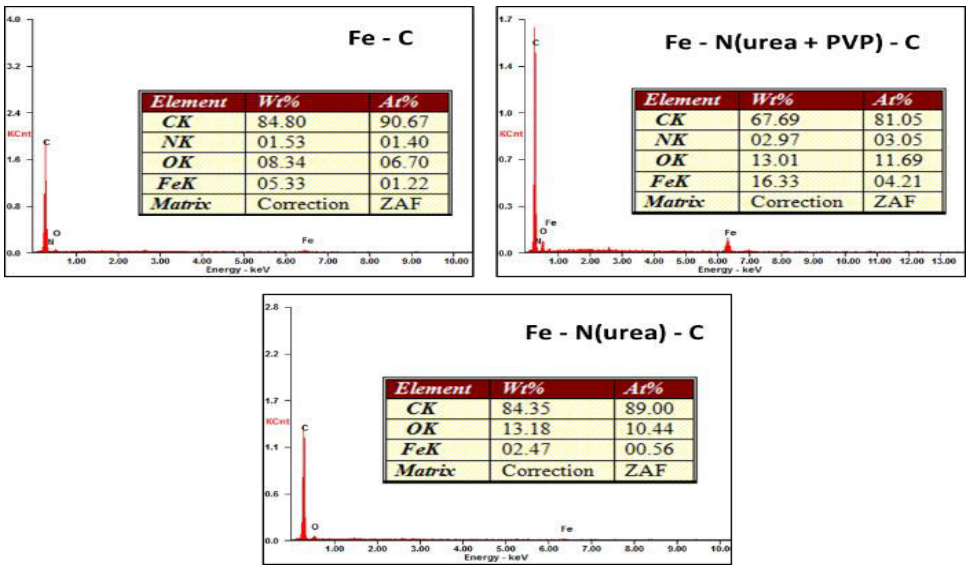

Figure-6. EDX data of obtained catalyst using various compositions nitrogen and carbon.

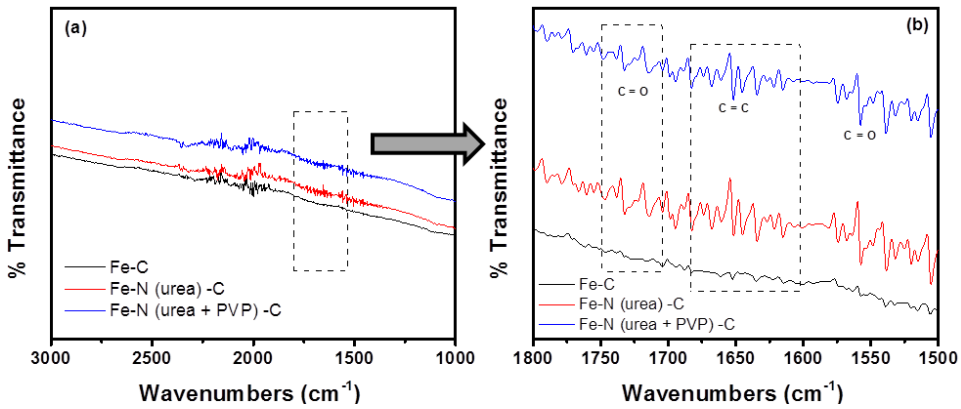

Figure-7. FTIR spectra of various catalysts using different nitrogen source.

The elemental content of the catalyst has the attributes to contribute good activity. Double nitrogen sources of Fe-N(urea+PVP)-C has the best electrochemical properties, due to the highest content of nitrogen and iron. Moreover, FTIR was used to determine the molecular structure of catalyst product. FTIR spectra of Fe-C, Fe-N(urea)-C, and Fe-N(urea+PVP)-C are combined in Figure-7. Strong peak of C=C and C=O clearly appear on the catalyst using nitrogen addition but do not exist in Fe-C. The noise peak of FTIR spectra on Fe-N(urea)-C and Fe-N(urea+PVP)-C shows that carbon bonding occurs after pyrolysis.

CONCLUSIONS

Nitrogen doping carbon on the catalyst gives a role to improve electrochemical properties, namely the value of capacitance that is increasing compared to only the content of Fe and C that make up the catalyst. The addition of double nitrogen produces the CV curve with the greatest capacitance. As for current density, nitrogen also has the effect of increasing the current density at the cathode during a reduction reaction. The amount of nitrogen in the catalyst with double nitrogen addition showed the highest nitrogen content in the EDX results. Fe-N (urea) -C catalyst has the highest surface area and the highest nitrogen content. Based on morphological observations through SEM images, it is known that the addition of nitrogen elements gives a smaller and evenly

distributed particle shape. This can be seen in the Fe-N (urea + PVP) -C catalyst which has a better particle distribution than Fe-C and Fe-N (urea) -C catalysts.

ACKNOWLEDGEMENTS

The financial support of the Ministry of Research Technology and Higher Education of Indonesia (113/SP2H/LT/DRPM/2019) as research funding for collaboration research scheme is acknowledged.

REFERENCES

[1] Z. Y. Sui *et al*. 2018. Nitrogen-doped and nanostructured carbons with high surface area for enhanced oxygen reduction reaction. Carbon N. Y. 126: 111-118.

[2] J. Snyder, T. Fujita, M. W. Chen and J. Erlebacher. 2010. Oxygen reduction in nanoporous metal-ionic liquid composite electrocatalysts. Nat. Mater. 9(11): 904-907.

[3] V. A. Setyowati, H. C. Huang, C. C. Liu and C. H. Wang. 2016. Effect of Iron Precursors on the Structure and Oxygen Reduction Activity of Iron–Nitrogen-Carbon Catalysts. Electrochim. Acta. 211(3): 933-940.

[4] K. Parvez *et al*. 2012. Nitrogen-Doped Graphene and Its Iron-Based Composite as Efficient Electrocatalysts for Oxygen Reduction Reaction. ACS Nano. 6(11): 9541-9550.

[5] N. Daems, X. Sheng, I. F. J. Vankelecom, and P. P. Pescarmona. 2014. Metal-free doped carbon materials as electrocatalysts for the oxygen reduction reaction. J. Mater. Chem. A. 2(12): 4085-4110.

[6] C. P. Ewels and M. Glerup. 2005. Nitrogen doping in carbon nanotubes. Journal of Nanoscience and Nanotechnology. 5(9): 1345-1363.

[7] R. Jäger *et al.* 2018. The effect of N precursors in Fe-N/C type catalysts based on activated silicon carbide derived carbon for oxygen reduction activity at various pH values. J. Electroanal. Chem. 823(April): 593-600.

[8] S. Yasuda, A. Furuya, Y. Uchibori, J. Kim and K. Murakoshi. 2016. Iron-nitrogen-doped vertically aligned carbon nanotube electrocatalyst for the oxygen reduction reaction. Adv. Funct. Mater. 26(5): 738-744.

[9] T. F. Hung *et al*. 2013. Influence of pyrolysis temperature on oxygen reduction reaction activity of carbon-incorporating iron nitride/nitrogen-doped graphene nanosheets catalyst. Int. J. Hydrogen Energy. 38(10): 3956-3962.

[10] C. Domínguez, M. A. Peña, S. Rojas and F. J. Pérez-Alonso. 2016. Effect of the pyrolysis atmosphere and nature of iron precursor on the structure and activity of Fe/N based electrocatalysts for the oxygen reduction reaction. Int. J. Hydrogen Energy. 41(47): 22560-22569.

[11] R. Cao et al. 2013. Promotion of oxygen reduction by a bio-inspired tethered iron phthalocyanine carbon nanotube-based catalyst. Nat. Commun. Vol. 4.

[12] S. Zhang, H. Zhang, X. Hua and S. Chen. 2015. Tailoring molecular architectures of Fe phthalocyanine on nanocarbon supports for high oxygen reduction performance. J. Mater. Chem. A. 3(18): 10013-10019.

[13] J. Herranz et al. 2011. Unveiling N-Protonation and Anion-Binding Effects on Fe/N/C Catalysts for O 2 Reduction in Proton-Exchange-Membrane Fuel Cells. J. Phys. Chem. C. 115(32): 16087-16097.

[14] G. Wu *et al*. 2011. Synthesis-structure-performance correlation for polyaniline-Me-C non-precious metal cathode catalysts for oxygen reduction in fuel cells. J. Mater. Chem. 21(30): 11392-11405.

[15] H. Kim, K. Lee, S. I. Woo and Y. Jung. 2011. On the mechanism of enhanced oxygen reduction reaction in nitrogen-doped graphene nanoribbons. Phys. Chem. Chem. Phys. 13(39): 17505-17510.

[16] L. Li, P. Dai, X. Gu, Y. Wang, L. Yan and X. Zhao. 2017. High oxygen reduction activity on a metal-organic framework derived carbon combined with high degree of graphitization and pyridinic-N dopants. J. Mater. Chem. A. 5(2): 789-795.

[17] M. Q. Wang, C. Ye, M. Wang, T. H. Li, Y. N. Yu and S. J. Bao. 2018. Synthesis of M (Fe3C, Co, Ni)-porous carbon frameworks as high-efficient ORR catalysts. Energy Storage Mater. 11(August 2017): 112-117.

[18] V. M. Bau, X. Bo, and L. Guo. 2017. Nitrogen-doped cobalt nanoparticles/nitrogen-doped plate-like ordered mesoporous carbons composites as noble-metal free

electrocatalysts for oxygen reduction reaction. J. Energy Chem. 26(1): 63-71.

[19] M. M. Hossen, K. Artyushkova, P. Atanassov and A. Serov. 2018. Synthesis and characterization of high performing Fe-N-C catalyst for oxygen reduction reaction (ORR) in Alkaline Exchange Membrane Fuel Cells. J. Power Sources. 375: 214-221.

[20] J. Zhang *et al*. 2015. Improved oxygen reduction activity of porous carbon materials by self-doping nitrogen derived from PVP with urea as a promoter. Electrochim. Acta. 177: 73-78.

[21] T. Yang *et al*. 2015. Hierarchical mesoporous yolk-shell structured carbonaceous nanospheres for high performance electrochemical capacitive energy storage. Chem. Commun. 51(13): 2518-2521.

[22] J. Zhang, S. Wu, X. Chen, M. Pan and S. Mu. 2014. Egg derived nitrogen-self-doped carbon/carbon nanotube hybrids as noble-metal-free catalysts for oxygen reduction. J. Power Sources. 271: 522-529.

[23] J. Liu, H. J. Choi and L. Y. Meng. 2018. A review of approaches for the design of high-performance metal/graphene electrocatalysts for fuel cell applications. J. Ind. Eng. Chem. 64: 1-15.

[24] J. Wang, S. Li, G. Zhu, W. Zhao, R. Chen and M. Pan. 2013. Novel non-noble metal electrocatalysts synthesized by heat-treatment of iron terpyridine complexes for the oxygen reduction reaction. J. Power Sources. 240: 381-389.

[25] V. A. Setyowati, D. Susanti, L. Noerochim, E. W. R. Widodo and M. Y. Sulaiman. 2019. Investigation of carbon composition for electrochemical properties as pemfc cathode catalyst. in Materials Science Forum. 964 MSF: 13-18.

[26] J. Zhang, D. He, H. Su, X. Chen, M. Pan and S. Mu. 2014. Porous polyaniline-derived FeNxC/C catalysts with high activity and stability towards oxygen reduction reaction using ferric chloride both as an oxidant and iron source. J. Mater. Chem. A. 2(5): 1242-1246.

[27] V. A. Setyowati *et al*. 2019. High oxygen reduction reaction activity on various iron loading of Fe-PANI/C catalyst for PEM fuel cell. Ionics (Kiel).

[28] D. Guo *et al*. 2018. In situ formation of iron-cobalt sulfides embedded in N, S-doped mesoporous carbon as efficient electrocatalysts for oxygen reduction reaction. Microporous Mesoporous Mater. 270: 1-9.